

An experimental study on drag forces on obstacles in granular flow.

Sounak Das¹, Deepika Chimote¹, Adarsh Kumar¹, Aqib Khan^{*}, Rakesh Kumar¹, and Sanjay Kumar¹

¹Department of Aerospace Engineering, Indian Institute of Technology, Kanpur, India

Abstract. The present work examines the interaction between granular flow and cylindrical obstacles. The experiments are conducted on an inclined chute where single or two cylinders are positioned at varying distances, with load cells to calculate drag forces and visualize shock wave behavior under different chute inclinations. The flow field is analyzed with high-resolution cameras and Particle Image Velocimetry (PIV) software, which enables precise tracking and measurement of flow patterns. When the grains interact with the cylinders, shock waves are produced on the upstream side, creating a grain-free zone in the downstream area. Additionally, the study investigates shock wave structures generated by both single and dual-cylinder configurations, revealing interesting patterns of shock-shock interactions and unique drag characteristics. This research addresses the formation of diffuse and bow shocks and explores how variables like chute inclination angle and Froude number influence the shock waves and drag forces. Drag measurements are obtained using a load cell mechanism.

1. Introduction

Granular matter consists of large particles that interact through friction and collisions leading to inelastic and dissipative behaviour. Their macroscopic size makes them athermal and the low speed of sound (~ 0.1 m/s) in such materials can generate shocks during flow (Khan *et al.* [1]). These shocks can be attached or detached depending on the obstacle shape and flow speed (Khan *et al.* [1]). Such shock behaviour can help divert avalanches making it important to understand the forces acting on obstacles. Wieghardt [2,3] showed that in quasi-static flows drag is mostly velocity-independent and governed by stress chain reorganization. In rotating beds at low Froude numbers drag scales with the square root of grain diameter due to depth-dependent friction. Albert *et al.* [4] further demonstrated linear scaling in a static bed, where drag arises from grain reorganization resisted by static friction. The difference in scaling reflects distinct regimes. In the rotating bed, drag scales with the square root of diameter due to depth-dependent friction, while in the static bed it scales linearly due to force chain reorganization resisting motion. It increases as grain size decreases and varies quadratically with flow depth. Atkinson *et al.* [5] found that Janssen's differential slice method overpredicts forces due to stress discontinuities and the method was later formalized by Nedderman [6]. Tüzün *et al.* [7] identified stagnation zones upstream and large voids downstream of square and triangular obstacles in dense granular flow. Chehata *et al.* [8] conducted 2D experiments on granular flow over a cylinder, determining that drag is velocity-independent. It increases nearly linearly with obstacle size and decreases with grain diameter. They

attributed the downstream granular vacuum to tensile stresses and insufficient granular temperature. Cui *et al.* [9] and Carvalho *et al.* [10] conducted an analysis on pinch-off and shock standoff distances in relation to the Froude number. They observed that when two intruders move close to each other in a granular medium, their motion becomes coupled, meaning the presence of one affects the forces on the other. This coupling reduces the average drag force on each intruder, facilitating easier movement compared to when they are isolated. They also proposed a predictive formula for flow height to prevent overtopping.

2. Experimental setup and Methodology

Figure 1 shows the schematic of the experimental setup. The experiment used transparent spherical soda-lime-silica grains with a diameter of $125 \mu\text{m}$ and a density of 1600 kg/m^3 . Grains were released from a hopper onto a rectangular glass chute measuring 310 mm wide and 1200 mm long. The chute was placed inside a channel mounted on an adjustable stand to vary the inclination angle ϕ , which was measured using an inclinometer and ranged from 15° to 40° . Cylindrical aluminium models, 50 mm in height and 20 mm to 60 mm in diameter (in 10 mm increments), were placed 750 mm from the hopper to act as obstacles. Drag force on each model was measured using a load cell system that included a bending beam load cell, microprocessor, battery, LED

^{*}Present address: Indian Institute of Science, Bangalore, India

display, L-bar, and shaft. The load cell measured forces from 20 mg to 1 kg. To test surface roughness effects, 80-grit coarse sandpaper sheets were applied to the glass surface to convert it from smooth to rough. The measured load (W) was converted into drag force (F_d) using the formula,

$$F_d = w \cdot g \quad (1)$$

where g represents the acceleration due to gravity. Measurements were conducted at various inclination angles (ϕ) and different lateral spacings to evaluate the drag force. In addition to calculating the drag, the variation in the Froude number with the channel inclination angle (ϕ) was also observed. The Froude number (F_r) is used to classify different flow regimes based on its value: subcritical flow occurs when $F_r < 1$, critical flow occurs when $F_r = 1$, and supercritical flow occurs when $F_r > 1$. The free-stream velocity was measured using particle image velocimetry (PIV) with images captured at 1500 fps using a high-speed camera. Image processing was done in MATLAB. Flow depth was measured using a micrometer with a least count of 0.01 mm. The flow initially appears as a thin sheet that thickens over time and reaches a steady level lasting around 7 to 8 seconds before it dissipates. At lower inclinations the grains move slowly and form a thick layer. As the angle increases the flow becomes faster and the layer thinner.

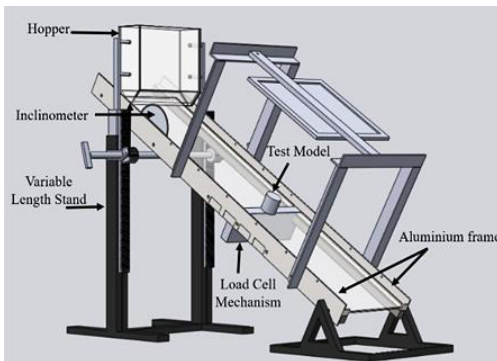


Fig. 1. Schematic of the experimental setup.

3. Results and Discussion

3.1 Drag on single cylinder.

Experiments are done on a single cylinder with different freestream velocities, which are attained by changing the inclination angle of the chute. Fig. 2 shows the flow dynamics as the grains pass over the cylindrical obstacle, depicting the dynamics of the granular bed. At lower inclination angles, it is seen that the flow is not fully retarded in front of the cylinder and forms a diffused shock. As the inclination angle is increased, the shock gets stronger and climbs up along the height of the cylinder. It is known that in a quasi-static regime, the drag is independent of the flow velocity, but in a non-

quasi-static regime, it can be seen in Fig. 3, that the drag varies with a change in inclination angle, i.e., it first decreases and then it increases after an inclination angle of around 24° , which is approximately equal to the grain-grain angle of repose. At low velocities, that is at lower inclination angles, the drag is due to the stagnation region upstream of the cylinder, the bigger the area, the more will be the drag. When the inclination angle increases, the grains fall off the cylinder, thus the size of the stagnation region decreases leading to a reduction in drag. As shown in Fig. 4, above 24° , the shock becomes sharper, which influences the physics of the granular flow. It is analogous to gas dynamics, that in high-speed flows, the prominent part of total drag is due to the shock waves, which is not the case in low-speed flows. It has been observed that drag increases when the inclination angle surpasses a critical point, known as the angle of repose between grains and surfaces. This occurs because shock standoff distance diminishes as the inclination angle rises. To compensate, the flow ascends along the cylinder's height, increasing the surface area in contact with the moving grains, commonly referred to as the wet surface area, and increasing drag in high-speed conditions. Additionally, in this high-speed regime, drag results from momentum transfer from grains to the cylinder. As the inclination angle grows, momentum exchange intensifies, further elevating drags in this scenario.

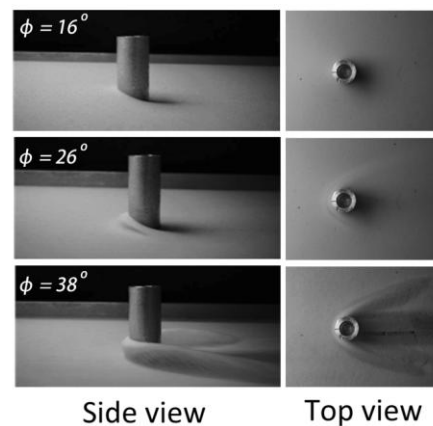


Fig. 2. Flow of grains over single cylinder at different inclinations over a smooth surface.

Now when the surface roughness is increased, the transition from viscous dominated flow to inertial dominated flow is delayed in terms of the inclination angle, as is shown in the Fig. 3. Here, the drag variation with different chute angles can be seen for different cylinder diameters. The behaviour is almost the same for both rough surface case and smooth surface case, but since a rough surface retards the flow, the occurrence of shock waves happens at a high angle of inclination. An interesting observation to make here is that the drag force for the rough channel is significantly different in magnitude from the drag force obtained with the smooth channel. Below a certain value of the channel inclination

($\phi < 25^\circ$), the drag force is higher for the rough channel, and vice-versa for higher values ($\phi > 25^\circ$). With this, one can conclude that the grain-surface angle of repose defines the critical angle to transit from the subcritical regime to the supercritical regime.

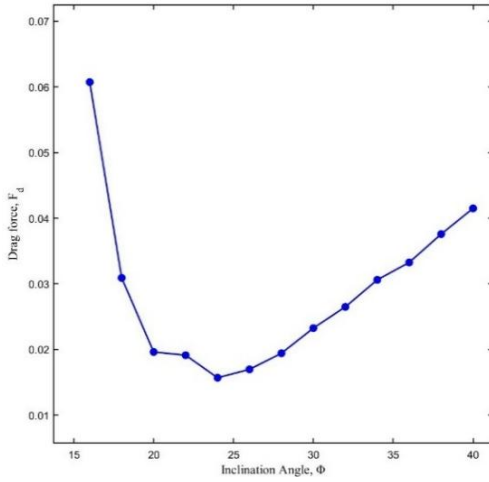


Fig. 3. Typical characteristics of drag force with the channel inclination for single cylinder over a smooth surface.

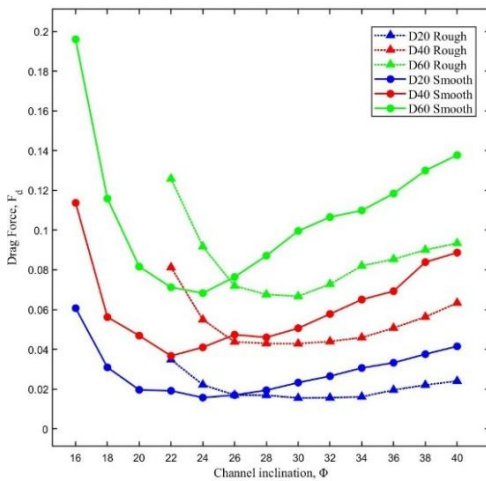


Fig. 4. Variation of drag for single cylinder of different diameters for different surface roughness. Sandpaper was used to create a rough surface

3.2 Drag on two cylinders

With the introduction of a second cylinder in the lateral direction of the flow, drag variation with inclination angle changes as compared to a single cylinder, as in Fig. 5. In the low-speed regime, drag initially decreases, similar to a single cylinder. However, in the high-speed regime, it saturates at a certain value. At lower inclination angles, the granular flow remains diffused, but as the angle increases, shocks form and become sharper. PIV analysis in Fig. 6 reveals that as inclination increases, the upstream stagnant region (blue) shrinks, reducing drag. Up to inclination angle of 26° , stagnation

remains upstream, but beyond this, flow localizes over the cylinders.

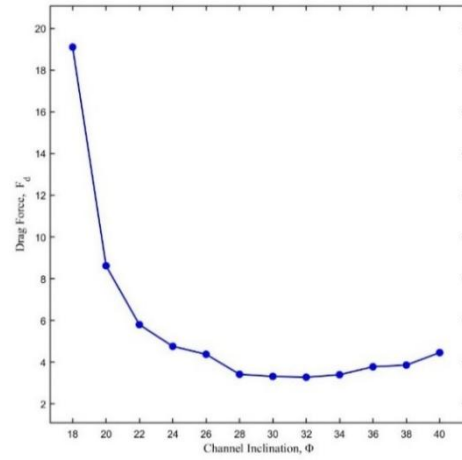


Fig. 5. Variation of drag force with inclination angle for two cylinders with 1D spacing between them over a smooth surface.

This shift occurs when the inclination angle of 26° matches the grain-grain angle of repose. Below it, the granular matter behaves like a solid; above it, it fluidizes and flows smoothly.



Fig. 6. PIV Images of shock interaction over cylinder ($D = 20$ mm) at various channel inclinations over a smooth surface.

It was also found that drag decreases with increasing inclination due to reduced flow depth, limiting the grains flowing over the cylinders. Experiments with different cylinder lateral spacings (Fig. 7) show a consistent trend: drag decreases with inclination until the critical angle, then rises. Surprisingly, at low angles, maximum drag occurs at 1.5D spacing, followed by 1D, 0D, and then 0.5D, rather than at 2D spacing. Non-dimensionalizing the drag force as the drag coefficient (C_d) and inclination angle as the Froude number (F_r) accounts for gravitational effects, merging variations due to different spacings into a single curve (Fig. 8). C_d is computed using Equation (2).

$$C_d = \frac{2F_d}{\rho v_{max} V_{\infty}^2 (2D)h} \quad (2)$$

Now variation of C_d for different spacings in between the cylinders is studied. It can be seen from the Fig. 8 that the drag coefficient follows a non-monotonic and seemingly random trend, decreasing in the order $1.5D$, $1D$, $0D$, $2D$, $0.5D$, and single cylinder at Froude number 1. Here, D denotes the diameter of the cylinder. Spacings such as $1.5D$ or $1D$ refers to center-to-center distances between adjacent cylinders, which are equal to 1.5 or 1 times the cylinder diameter, respectively. At low inclination angles the drag is mainly due to the stagnant region that forms in front of the cylinder and also because the grains move collectively as a solid-like mass until a critical angle is reached. In this state the granular material shows little internal movement and the particles shift together like a rigid block. Force transmission happens through stable contact networks called stress chains. As the inclination increases beyond a critical angle the material begins to deform and flow more freely. When spacing is large, drag is due to shock interactions.

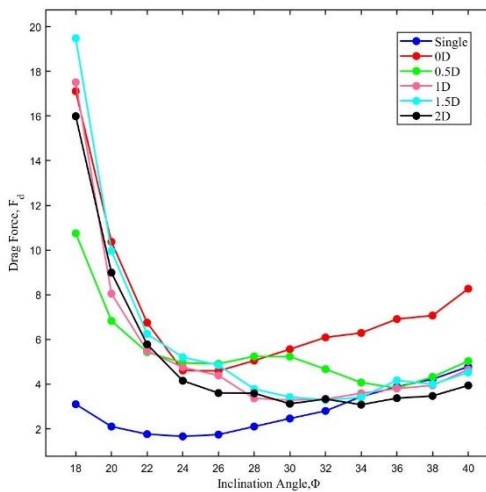


Fig. 7. Variation of F_d with ϕ for different lateral spacings in two cylinders configuration over a smooth surface.

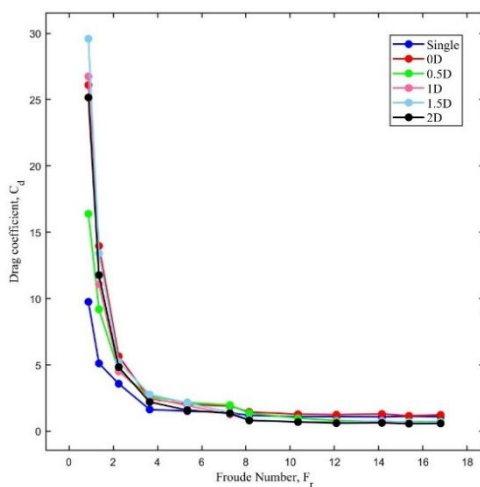


Fig. 8. Variation of drag coefficient, C_d with Froude number, F_r for two cylinders configuration kept at different lateral spacings over a smooth surface.

4. Conclusion

This study examines drag force on cylinders in granular flow, focusing on shock wave interactions with inclination angle (ϕ) in gravity-driven open-channel flow. Cylinders placed in granular flow experience different shock fronts. Diffuse shocks develop in slow, dense flows with Froude numbers between 0.5 and 4, while bow shocks emerge in rapid, dilute flows ranging from 5 to 18. As Froude number increases, the drag coefficient gradually decreases and stabilizes at higher values, indicating a trend where drag force approaches a steady state in high-speed granular flows. These findings enhance the understanding of drag mechanisms in granular systems and their similarities to fluid dynamics, offering insights into shock interactions problems.

5. Reference

1. A.Khan, P.Hankare, S.Verma, Y.Jaiswal, R.Kumar, S.Kumar, Detachment of strong shocks in confined granular flows. *J. Fluid Mech.* **935**, A13 (2022). <https://doi.org/10.1017/jfm.2022.5>
2. K. Wiegardt, Experiments in granular flow. *Annu. Rev. Fluid Mech.* **7.1**, 89–114 (1975). <https://doi.org/10.1146/annurev.fl.07.010175.000513>
3. K. Wiegardt, Forces in granular flow. *Mech. Res. Commun.* **1**, 3–7(1974). [https://doi.org/10.1016/0093-6413\(74\)90027-5](https://doi.org/10.1016/0093-6413(74)90027-5)
4. R. Albert, M.A.Pfeifer, A.L. Barabási, P. Schiffer, Slow drag in a granular medium. *Phys. Rev. Lett.* **82**, 205 (1999). <https://doi.org/10.1103/PhysRevLett.82.205>
5. T. Atkinson, J. Butcher, J.C. Butcher, M.J. Izzard, R.M. Nedderman, the forces on obstacles suspended in flowing granular materials. *Chem. Eng. Sci.* **38**, 91–105 (1983). [https://doi.org/10.1016/0009-2509\(83\)80138-9](https://doi.org/10.1016/0009-2509(83)80138-9)
6. R.M. Nedderman, Statics and kinematics of granular materials (Cambridge University press., 1992) <https://doi.org/10.1017/CBO9780511600043>
7. U. Tüzün, R.M. Nedderman, Gravity flow of granular materials round obstacles-II: investigation of the stress profiles at the wall of a silo with inserts. *Chem. Eng. Sci.* **40**, 337–351 (1985). [https://doi.org/10.1016/0009-2509\(85\)85096-X](https://doi.org/10.1016/0009-2509(85)85096-X)
8. D. Chahata, R. Zenit, C.R. Wassgren, Dense granular flow around an immersed cylinder. *Phys. Fluids* **15**, 1622–1631 (2003). <https://doi.org/10.1063/1.1571826>
9. X. Cui, Gravity-driven granular free-surface flow around a circular cylinder. *J. Fluid Mech.* **720**, 314–337 (2013).
10. D.D. Carvalho, Y. Bertho, A. Seguin, E.M. Franklín, B. Darbois, Drag reduction during the side-by-side motion of a pair of intruders in a granular medium. *Phys. Rev. Fluids* **9**, 114303 (2024). <https://doi.org/10.1103/PhysRevFluids.9.114303>